PHYSICAL REVIEW C VOLUME 58, NUMBER 1 JULY 1998

Sideways-peaked angular distributions in hadron-induced multifragmentation: Shock waves, geometry, or kinematics?

W.-c. Hsi, K. Kwiatkowski, G. Wang,* D. S. Bracken,† E. Cornell,‡ D. S. Ginger,§ V. E. Viola, and N. R. Yoder
Department of Chemistry and IUCF, Indiana University, Bloomington, Indiana 47405

R. G. Korteling
Department of Chemistry, Simon Fraser University, Burnaby, British Columbia, Canada V5A 1S6

F. Gimeno-Nogues, E. Ramakrishnan, D. Rowland, and S. J. Yennello
Department of Chemistry and Cyclotron Institute, Texas A & M University, College Station, Texas 77843

R. Huang, W. G. Lynch, M. B. Tsang, and H. Xi
Department of Physics and NSCL, Michigan State University, East Lansing, Michigan 44824

H. Breuer
Department of Physics, University of Maryland, College Park, Maryland 20742

K. B. Morley
Los Alamos National Laboratory, Los Alamos, New Mexico 87545

S. Gushue and L. P. Remsberg
Chemistry Department, Brookhaven National Laboratory, Upton, New York 11973

W. A. Friedman
Department of Physics, University of Wisconsin, Madison, Wisconsin 53706

A. Botvina
Department of Physics, Bologna University, Bologna 40126, Italy

(Received 19 March 1998)

Exclusive studies of sideways-peaked angular distributions for intermediate-mass fragments (IMFs) produced in hadron-induced reactions have been performed with the Indiana silicon sphere (ISiS) detector array. The effect becomes prominent for beam momenta above about 10 GeV/c. Both the magnitude of the effect and the peak angle increase as a function of fragment multiplicity and charge. When gated on IMF kinetic energy, the angular distributions evolve from forward peaked to nearly isotropic as the fragment energy decreases. Fragment-fragment correlation studies show no evidence for a preferred angle that might signal a fast dynamic breakup mechanism. Moving-source and intranuclear cascade simulations suggest a possible kinematic origin arising from significant transverse momentum imparted to the recoil nucleus during the fast cascade. A two-step cascade and statistical multifragmentation calculation is consistent with the data. [S0556-2813(98)50707-8]

PACS number(s): 25.40.Ve, 21.65.+f, 25.70.Pq, 25.75.−q

A longstanding puzzle in understanding interactions between GeV protons and heavy target nuclei is the observation of sideways-peaked angular distributions for complex fragments [1–3]. For incident energies below about 5 GeV, the inclusive angular distributions are forward peaked [4–6] and can be accounted for as a superposition of two average sources: one that retains the memory of the incident beam and a second that resembles a slowly moving equilibrated residue [7], or a distribution of moving equilibriated sources [6]. In the incident energy interval between 5–10 GeV, a transition from forward-to-sideways peaking develops in the angular distributions for intermediate-mass fragments (IMF: $3 = z \lesssim 15$). At the same time, the IMF cross sections [8] and deposition energy [9] become nearly independent of bombarding energy and a distinct change in the character of the energy spectra is observed [5,8,10], signaling the onset of multifragmentation. In fact above about 5 GeV, the angular distributions are the only IMF reaction observable that appears to exhibit appreciable sensitivity to beam energy.

Several interpretations of sideways peaking observed in the inclusive IMF studies of Refs. [1–3] have been proposed. Remsberg and Perry [1] noted that the peak in the IMF an-

*Present address: H. K. Systems, Inc., Milwaukee, WI.
†Present address: Los Alamos National Laboratory, Los Alamos, NM 87545.
‡Present address: Lawrence Berkeley Laboratory, Berkeley, CA 94720.
§Present address: Cambridge University, Cambridge, England.

gular distributions near 60°–70° coincided with about the same angle predicted for light particles ejected from a nuclear shock wave [11]. Fortney and Porile [2] accounted for similar results in terms of a one-step mechanism based on a coherent flux model [12]. In contrast, Urbon *et al.* [3] explained their results with a two-step model involving a fast cascade followed by decay of a hot residue. Wilkins *et al.* [13] and Hüfner *et al.* [14] subsequently proposed that sideways peaking with GeV hadron beams could be understood in terms of a nuclear cleavage model in which the leading hadron creates a cylindrical low-density region in its wake. Large transverse momentum transfer and Coulomb forces then act to focus the fragments transverse to the beam axis. More recently, coincidence studies in a planar geometry with 12-GeV protons [15] suggested that sideways peaking for heavier IMFs was enhanced when a second IMF was detected near 90° on the opposite side of the beam axis. It was suggested that this observation might be due to a fast multifragmentation of a toroid-shaped residue, as predicted by a QMD calculation [16].

Recent Boltzmann-Uehling-Uhlenback (BUU) calculations provide support for the possible role of dynamics in destabilizing heavy residues formed in central collisions induced by GeV hadrons [17]. First, as the projectile and its associated momentum front punches through the nucleus, significant mass loss occurs, creating conditions favorable to development of an acoustic-type shock wave with low compression ($\rho/\rho o \sim 1.3$). Second, a significant depletion of nucleons in the nuclear core is predicted to evolve near the end of the fast cascade, creating a temporary bubblelike geometry in the hot residue with density ($\rho/\rho o \leq 0.7$), near the spinodal region. How the cohesive nuclear forces respond to these rapid perturbations and whether sideways peaking is a manifestation of such effects is a central question in distinguishing between dynamically-driven and purely thermal multifragmentation. This question has also been examined recently in the context of the intranuclear cascade model [18]. To this end, in this Rapid Communication we describe exclusive 4π studies that provide the first opportunity to examine the sideways-peaking phenomenon as a function of fragment correlation angles, multiplicity, charge, and kinetic energy over a range of projectile energies spanning the transition region from forward to sideways peaking.

The experiment was performed with the Indiana silicon sphere (ISiS) 4π detector array [19] at the Brookhaven AGS accelerator (E900). Secondary positive beams of momentum 6.0, 10.0, 12.8, and 14.6 GeV/c and negative beams at 5.0, 8.2, and 9.2 GeV/c were incident on a 1.8 mg/cm^2 ^{197}Au target. Positive beams are associated with protons and negative beams with π^- projectiles. Identified light charged particles ($^{1-3}$H and ^{3,4}He isotopes) and IMFs up to $Z \leq 16$ were detected with the ISiS array, which consisted of 162 telescopes containing gas-ionization chamber, silicon, and CsI detector elements. The telescopes spanned the angular range 14°–86.5° and 93.5°–166°, corresponding to a solid angle coverage of about 70%. The energy acceptance for Z identification was $1.0 \leq E/A \leq 95$ MeV. The hardware multiplicity trigger required signals in three or more silicon detectors in the array. Results obtained with this minimum-bias trigger are referred to as ''inclusive'' in this paper. Additional details of the experiment are given in Ref. [9].

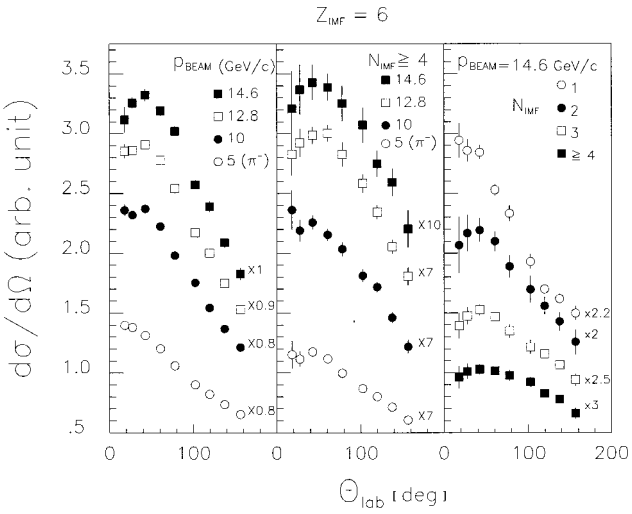

FIG. 1. Angular distributions of carbon fragments from a ^{197}Au target. Left frame: inclusive data for 10.0, 12.8, and 14.6 GeV/c protons and 5.0 GeV/c π^-; center: data for the same beam momenta gated on IMF multiplicity $N_{IMF} \geq 4$; and right: 14.6 GeV/c proton data gated on IMF multiplicity. Legends on the figures identify curves; relative cross sections are indicated by scale factors associated with each angular distribution.

In Fig. 1 several qualitative features of the angular distributions are shown. Data are for carbon fragments, which are representative of all $Z \geq 5$ fragments. While the sideways-peaking effect is small (~20%), it is a systematic feature of the data. In the left-hand frame, the inclusive angular distributions are shown for 10.0, 12.8, and 14.6 GeV/c protons and 5.0 GeV/c pions. The 5.0 GeV/c π^- data are similar to those for 6.0 GeV/c protons and the two higher-momenta π^- measurements are intermediate between the 6.0 and 10.0 GeV proton results. The forward-to-sideways-peaked evolution of the angular distributions with beam momentum is apparent in Fig. 1. In the center frame, angular distributions for carbon fragments gated on IMF observed multiplicity $N_{IMF} \geq 4$ are shown for the same incident conditions, i.e., 5.0 GeV/c π^- and 10.0, 12.8, and 14.6 GeV/c protons. Here one observes the same systematic trend as the inclusive data, with the peak shifted toward larger angles. In addition, when high multiplicity events are selected, a flattening of the 5.0 GeV/c π^- angular distribution develops.

In the right-hand frame of Fig. 1, angular distributions at 14.6 GeV/c beam momentum are plotted as a function of observed IMF multiplicity. For $N_{IMF} = 1$, the results are similar to inclusive measurements at 5 GeV/c and below [7]. With increasing N_{IMF}, the peak angle shifts to larger angles and the peak-to-backwardmost-angle ratio decreases (from 2.0 to 1.5). Similar trends are observed for the 12.8 and 10.0 GeV/c proton beams, although less pronounced. Thus the results in Fig. 1 indicate that the observed sideways peaking above 10 GeV is primarily associated with high deposition-energy multifragmentation events.

A signature of the shock wave or toroidal-breakup mechanisms would be the observation of events with enhanced multiplicity for fragments emitted into the same angular interval, e.g., in an annulus about the beam axis. To test this scenario, we examined angular-correlations $C(\theta_t, \theta_g)$ between coincident IMFs. For reference, the ISiS array is com-

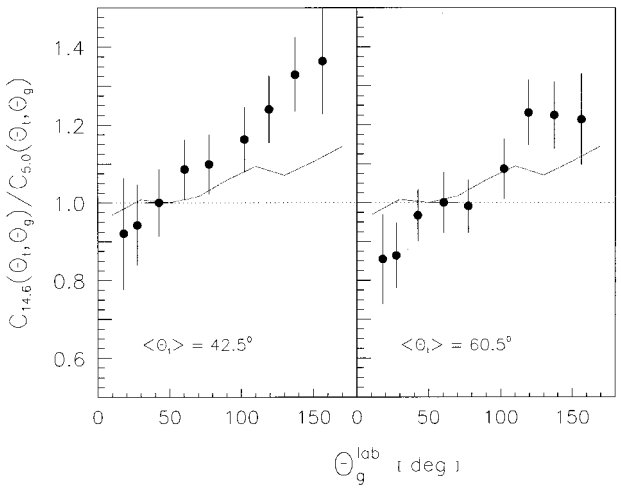

FIG. 2. Relative correlation probability (points) for coincident pairs of IMFs produced in $N_{IMF} \geqslant 3$ events from the 14.6 GeV/c p + Au reaction, gated on the annular intervals 33°–52° (left) and 52°–69° (right). Correlations are normalized to an identical analysis for $N_{IMF}=2$ for the 5.0 GeV/c π^- data. IMF acceptance was $Z=4-12$ and $E/A=1-4$ MeV for the trigger and $E/A=1-8$ MeV for correlated IMFs. The solid line is the prediction of a hybrid INC and SMM [26] calculation.

posed of nine concentric annular rings, each corresponding to a fixed polar angle and containing 18 azimuthal telescope segments. The analysis focused on situations in which θ_t was associated with IMFs observed in each of the two polar-angle intervals, where the maximum in the angular distributions is observed, 33°–52° and 52°–69°. (These are defined here as ''trigger fragments'' and the angular interval as ''trigger interval.'') For each of these angles θ_t the dependence on the angle of the remaining $(N_{IMF}-1)$ IMFs θ_g was studied (these fragments are defined as ''global fragments''). The IMF acceptance included $Z=4-12$ fragments for events with $N_{IMF} \geqslant 3$ with kinetic energy $E/A=1-4$ MeV for the trigger fragments and $E/A=1-8$ MeV for the global IMFs. These events exhibit the highest probability for sideways peaking, discussed further below. Inclusion of all $E/A=1-8$ MeV fragments in the ''trigger interval'' does not change the results.

The global correlations are found to be similar for both trigger intervals. Rather than showing an enhancement, there is a factor of 2–3 suppression for IMF-IMF correlations within each trigger interval. Thus, there is no definitive signal for enhanced IMF emissions in the angular region where sideways peaking is found. In order to investigate this conclusion further, the correlations for 14.6 GeV/c proton data with $N_{IMF} \geqslant 3$ have been normalized to a similar correlation analysis for the 5.0 GeV/c π^- data; for the reference correlation, all events with $N_{IMF}=2$ were accepted to insure comparison with a monotonically decreasing angular distribution. In this way uncertainties due to solid angle, detector thresholds and target shadowing are minimized. As shown in Fig. 2, this analysis also fails to provide evidence for preferential emission of the fragments in any given angular region. The only obvious trend in Fig. 2 is the systematic increase in relative correlation probability with an increasing angle, which arises from the increasingly isotropic nature of the angular distributions as the beam momentum increases. This suggests that IMF emission is primarily influenced by Coulomb repulsion effects and global momentum conservation associated with the recoil nucleus and its fragmentation products. For each of the polar-angle intervals, azimuthal correlations have been examined ($\theta_t=\theta_g$). For both trigger and global intervals we find that the maximum correlation occurs when the two fragments are separated by 180° in azimuthal angles, consistent with the above arguments vis-à-vis Coulomb and momentum-conservation effects.

In addition, a sphericity and coplanarity analysis [20] has been performed on the 5.0 GeV/c π^- and 14.6 GeV/c proton data for thermal-like IMFs and light charged particles. For the high IMF multiplicity events the average sphericity is $\langle S \rangle \sim 0.50-0.60$ and the coplanarity is $\langle C \rangle \lesssim 0.10$. These values are nearly the same for both beam energies and are consistent with previous results for the 4.8 GeV ^{3}He+^{197}Au system, where no sideways peaking was observed [21,22]. The multiplicity distributions for $E/A=1-4$ MeV ejectiles have also been compared for the same polar angle intervals in the forward and backward hemispheres. These are identical within statistics. Thus, no statistically meaningful signature for dynamical production of IMFs because of a collective shock wave or a geometrically-unstable configuration is apparent in these analyses. The two-body cleavage mechanism [13,14] is more difficult to assess because of the multiplicity-three trigger condition and the 1 MeV/nucleon threshold of the ISiS array. However, no change in the coplanarity $\langle C \rangle$ is observed in the data, which might be expected if fissionlike events from a compact shape were present in a significant yield.

In order to gain further insight into the origin of the sideways-peaking effect, the dependence of the angular distributions on IMF charge and kinetic energy have been investigated. For the 5.0 GeV/c π^- data, the forward-peaked angular distributions exhibit nearly identical slopes for all IMF Z values. At 14.6 GeV/c, however, there is a distinct evolution of the peak angle towards larger angles and a weak trend towards increasing isotropy as the IMF charge increase. This effect has also been noted in the inclusive studies of Refs. [1–3], as well as for heavier fragments in radiochemical heavy-ion studies [23].

The most striking feature of the angular distributions is the dependence on IMF kinetic energy. Figure 3 shows the angular distributions of $Z=5-9$ fragments with energy cuts of $E/A=1.2-3$, 3–5, and 5–10 MeV, respectively, for 5.0 GeV/c π^- (left) and 14.6 GeV/c proton beams (center). Data are for $N_{IMF} \geqslant 3$ and are normalized to the backward-most point. It should be emphasized that the IMF yield is largest for the lowest E/A bin. This plot demonstrates that as the IMF velocity decreases, the maximum differential cross section evolves towards more backward angles and the overall angular distribution becomes more isotropic.

The observation that sideways emission is favored by increasing IMF masses and low kinetic energies suggests a possible kinematic origin for the effect. The diffractive nature of the initial N-N collision preferentially produces a secondary nucleon or N^* that recoils at 70°–90° [24]. Thus, subsequent dissipation during the cascade imparts a significant transverse velocity to the heavy residue. This is confirmed by intranuclear cascade calculations (INC) [25,26] in Fig. 4, where the distribution of longitudinal versus trans-

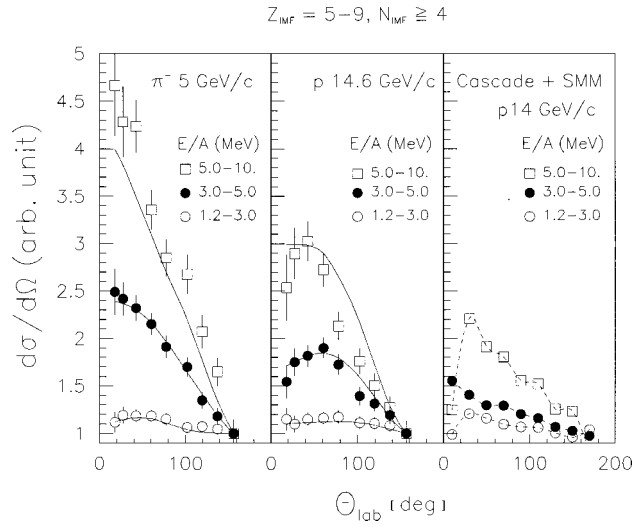

FIG. 3. Relative angular distributions as a function of IMF kinetic energy for $Z=5-9$ fragments from events with IMF multiplicity $N_{IMF}\geqslant 3$ from 5 GeV/c π^- (left) and 14.6 GeV/c proton (center) reactions on ^{197}Au. Data are gated on fragment E/A, as indicated. The absolute yield for each kinetic-energy cut decreases with increasing fragment E/A value. Solid lines are the result of a two-component moving-source fit to the data. The right-hand frame shows predictions of an INC and SMM hybrid calculation of the angular distributions for 14.6 GeV/c protons, gated on fragment energy (symbols and dashed line). All distributions are normalized to unity at the most backward angle.

verse velocity ($v_\parallel$ vs $v_\perp=\sqrt{v_x^2+v_y^2}$) is plotted for recoils with excitation energies $E^*>500$ MeV produced in the 14.6 GeV/c $p+$Au reaction. Cascade simulations were performed with a random impact parameter ($\langle b\rangle=3.5$ fm is predicted by the code). Transverse velocities up to 1 cm/ns are predicted for the heavy residues, with a significant fraction recoiling into the backward hemisphere. The effect of the heavy residue velocity vector on the resultant IMF vector is largest for the lower-energy IMFs ($v=1.5-2.5$ cm/ns) where the cross sections are also the largest. This nonaxial component of the recoil velocity vector can perturb the angular distributions significantly. The inset in Fig. 4 shows INC predictions of the average velocity vector $\langle v_R\rangle$ for residues with $E^*>500$ MeV produced with 600 MeV to 90 GeV hadron beams incident on ^{197}Au. With an increasing beam energy, $v_\perp$ becomes increasingly important and the distributions broaden significantly. The most rapid growth occurs between 1.0–5.0 GeV, followed by a nearly constant value above 10 GeV.

The effect of the residue recoil angle on the angular distributions of IMFs has been verified by performing a one-component moving-source simulation that imposes isotropic breakup kinematics. For residue recoil angles of about 60° or less with respect to the beam, only a monotonically-decreasing angular distribution results, i.e., no sideways peaking. This is consistent with the observation of such angular distributions at incident energies below 5 GeV, where the INC simulations also predict smaller, more forward-peaked recoil momenta. On the other hand, once the most probable recoil angle evolves beyond about 60°, the coupling of the residue and the IMF velocity vectors produces sideways-peaked angular distributions. Thus the distribution of recoil angles for the residues strongly influences the probability for sideways peaking in the laboratory system.

We have also performed a simple two-component moving-source fit to the measured spectra, assuming one source is moving in the beam direction and the second is focused at some average angle, determined by the fit. Both sources assume isotropic emission in the source frame. The results are shown in Fig. 3 for $Z=5-9$ fragments emitted from $N_{IMF}\geqslant 3$ events for the 5 GeV/c π^- and 14.6 GeV/c proton reactions. The transverse source accounts for about 80% of the yield at the higher beam momentum, but only about 25% for the lower beam momentum. This fit yields an

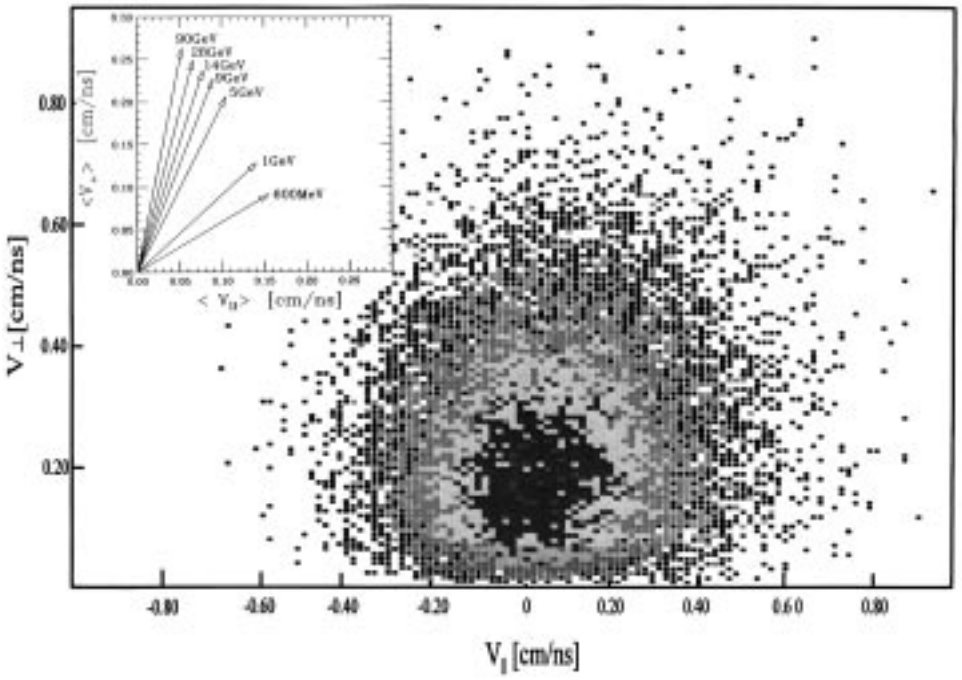

FIG. 4. Intranuclear cascade calculations showing the distribution of longitudinal versus perpendicular velocity for residues with excitation energies $E^*>500$ MeV formed in the 14 GeV $p+$Au reaction. Inset shows INC predictions of the average residue velocity vector $\langle V_\parallel\rangle$ vs $\langle V_\perp\rangle$ plane for, clockwise, 600 MeV, 1 GeV, 5 GeV, 9 GeV, 14 GeV, 28 GeV, and 90 GeV protons incident on a Au nucleus.

average recoil angle of $\theta \sim 80°$ for the 14.6 GeV/c data. Combined, the two sources give a satisfactory fit to the data.

To simulate the combined effects of recoil angle and statistical breakup, we have examined the angular distributions predicted by a hybrid intranuclear cascade and statistical multifragmentation model (SMM) [26]. Such a model should provide a schematic picture of the combined influence of the fast cascade and statistical multifragment breakup on the angular distributions. We have summed all IMFs $Z=5-9$ to improve statistics. In Fig. 2 the model predictions are compared with the relative correlation results, normalized to each of the trigger angular intervals. A qualitative consistency is observed. The inclusion of forward-peaked nonequilibrium light-charged-particle and IMF emission in the model would improve the agreement. The right-hand panel of Fig. 3 shows the predicted angular distributions for IMFs with $E/A = 1.2-3$, 3–5, and 5–10 MeV. The latter comparison demonstrates that significantly greater isotropy is expected for the low-energy IMFs relative to those with higher energies. Accounting for prebreakup IMF emissions ($\sim 10-15\%$ of the yield) would further increase the forward peaking of the most energetic component. These same arguments serve to explain the increase in the peak angle as a function of IMF charges, since the average velocity of the fragments decreases with increasing Z. Thus, the simulation is consistent with a two-step mechanism in which kinematic focusing of IMFs emitted from a hot residue with significant transverse momentum produces a sideways peak in the angular distributions.

In summary, we have performed exclusive studies that investigate the origin of sideways peaking of IMFs produced in hadron-heavy nucleus collisions. The effect becomes important above about 10 GeV/c and is found to be most pronounced for high-multiplicity, low kinetic-energy multifragmentation events. The peak angle increases with increasing beam energy and IMF charge. Investigations of IMF-IMF angular correlations, multiplicity distributions, and sphericity and coplanarity distributions provide no ''smoking gun'' that would support arguments for dynamical effects such as shock waves or toroidal-breakup mechanisms. Instead, it appears that the sideways peaking of IMFs can originate in kinematic-focusing effects associated with statistical and thermal multifragmentation of an expanding residue having a significant velocity component transverse to the beam axis. This is consistent with the observation that all other multifragmentation observables are insensitive to beam energy above about 5 GeV. Thus, if dynamical effects are present in the IMF data, they exist on a background in which kinematic focusing of heavy recoils cannot be ignored.

The authors wish to thank Wolfgang Bauer, Pawel Danielewicz, and Scott Pratt for discussions concerning these results. The assistance of Hugh Brown, John Gould, Bill McGahern and Phil Pile at AGS was vital to the successful completion of these experiments. One of us (W.A.F.) acknowledges the support of the Indiana University Institute for Advanced Study. Support for this research was provided by the U.S. Department of Energy, the National Science Foundation, and the National Research Council of Canada.

[1] L. P. Remsberg and D. G. Perry, Phys. Rev. Lett. **35**, 361 (1975).
[2] D. R. Fortney and N. T. Porile, Phys. Lett. **76B**, 553 (1978).
[3] J. Urbon, S. B. Kaufman, D. J. Henderson, and E. P. Steinberg, Phys. Rev. C **21**, 1048 (1980).
[4] J. B. Cumming, R. J. Cross, Jr., J. Hudis, and A. M. Poskanzer, Phys. Rev. **134**, B167 (1964).
[5] A. M. Poskanzer, G. W. Butler, and E. K. Hyde, Phys. Rev. C **3**, 882 (1971).
[6] R. E. L. Green and R. G. Korteling, Phys. Rev. C **22**, 1594 (1980).
[7] G. D. Westfall, R. G. Sextro, A. M. Poskanzer, A. M. Zebelman, and G. W. Butler, Phys. Rev. C **17**, 1368 (1978).
[8] N. Porile *et al.*, Phys. Rev. C **39**, 1914 (1989).
[9] W.-c. Hsi *et al.*, Phys. Rev. Lett. **79**, 817 (1997).
[10] S. J. Yennello, K. Kwiatkowski, S. Rose, L. W. Woo, S. H. Zhou, and V. E. Viola, Phys. Rev. C **41**, 79 (1990).
[11] A. E. Glassgold, W. Heckrottle, and K. M. Watson, Ann. Phys. (N.Y.) **6**, 1 (1959).
[12] K. Gottfried, Phys. Rev. Lett. **32**, 957 (1974).
[13] B. D. Wilkins, S. B. Kaufman, and E. P. Steinberg, Phys. Rev. Lett. **43**, 1080 (1979).
[14] J. Hüfner, Phys. Rep. **124**, 130 (1985); S. Bohrman, J. Hüfner, and M. C. Nemes, Phys. Lett. **120B**, 59 (1983).
[15] K. H. Tanaka *et al.*, Nucl. Phys. **A583**, 581c (1995).
[16] T. Maruyama and K. Nitia, Prog. Theor. Phys. **97**, 579 (1997).
[17] G. Wang, K. Kwiatkowski, V. E. Viola, W. Bauer, and P. Danielewicz, Phys. Rev. C **53**, 1811 (1996).
[18] M. Colonna *et al.* Phys. Rev. C **55**, 1404 (1997).
[19] K. Kwiatkowski *et al.*, Nucl. Instrum. Methods Phys. Res. A **360**, 571 (1995).
[20] G. Fai and J. Randrup, Nucl. Phys. **A404**, 551 (1983); J. A. Lopez and J. Randrup, *ibid.* **A491**, 477 (1989).
[21] E. Renshaw Foxford *et al.*, Phys. Rev. C **54**, 749 (1996).
[22] K. B. Morley *et al.*, Phys. Rev. C **54**, 737 (1996).
[23] W. Loveland, K. Aleklett, R. Yanez, A. Srivastava, and J. O. Liljenzin, Phys. Lett. B **312**, 53 (1993).
[24] H. Araseki and T. Fujita, Nucl. Phys. **A399**, 434 (1983).
[25] V. Toneev, N. S. Amelin, K. K. Gudima, and S. Yu. Sivoklokov, Nucl. Phys. **A519**, 463c (1990).
[26] A. Botvina, A. S. Iljinov, and I. N. Mishustin, Nucl. Phys. **A507**, 649 (1990).